









Material and Structural Characterization of a Wind Turbine Blade for Use as a Bridge Girder

 Transportation Research Record
1–9

 © National Academy of Sciences:
Transportation Research Board 2022
Article reuse guidelines:

sagepub.com/journals-permissions
DOI: 10.1177/03611981221083619

journals.sagepub.com/home/trr


Kieran Ruane¹, Zoe Zhang² , Angela Nagle³ , An Huynh⁴ ,
Ammar Alshannaq² , Asha McDonald⁵, Paul Leahy³ , Marios Soutsos⁴ ,
Jennifer McKinley⁴ , Russell Gentry⁵, and Lawrence Bank⁵ 

Abstract

Fiber reinforced polymer (FRP) composite materials have been used in a variety of civil and infrastructure applications since the early 1980s, including in wind turbine blades. The world is now confronting the problem of how to dispose of decommissioned blades in an environmentally sustainable manner. One proposed solution is to repurpose the blades for use in new structures. One promising repurposing application is in pedestrian and cycle bridges. This paper reports on the characterization of a 13.4-m long FRP wind blade manufactured by LM Windpower (Kolding, Denmark) in 1994. Two blades of this type were used as girders for a pedestrian bridge on a greenway (walking and biking trail) in Cork, Ireland. The as-received geometric, material, and structural properties of the 27-year-old blade were obtained for use in the structural design of the bridge. The material tests included physical (volume fraction and laminate architecture) and mechanical (tension and compression) tests at multiple locations. Full-scale flexural testing of a 4-m long section of the blade between 7 and 11 m from the root of the blade was performed to determine the load-deflection behavior, ultimate capacity, strain history, and failure modes when loaded to failure. Key details of the testing and the results are provided. The results of the testing revealed that the FRP material is still in excellent condition and that the blade has the strength and stiffness in flexure to serve as a girder for the bridge constructed.

Keywords

infrastructure, structures, innovative highway structures and appurtenances, FRP

The Re-Wind Network (www.re-wind.info) is a network consisting of five universities and industry affiliates in the United States, UK, and Ireland that conducts research on the repurposing of fiber reinforced polymer (FRP) composite wind turbine blades. The network has been in operation since 2017 and has published conceptual repurposing design catalogs (1, 2). Several of these concepts have been developed in greater detail: affordable housing (3), pedestrian bridges (4), and transmission power poles (5). The Re-Wind Network is currently designing and constructing two full-scale demonstration wind blade repurposing projects: a power pole prototype is being constructed in Kansas, in the United States, and a pedestrian bridge prototype was constructed in Cork, Ireland. This paper discusses the experimental characterization of a wind blade used as a girder in the Cork bridge.

FRP composite materials are not biodegradable and present unique problems for waste management at their

end-of-life (EOL). The impact of polymers on the environment and society has become a major concern in many countries. In response to the European Directive (6), the option of disposing of EOL FRP blades in landfills is now restricted by landfill bans or taxes and reuse, recycling, and recovery targets. Since the 1990s, there

¹Department of Civil, Structural and Environmental Engineering, Munster Technological University, Cork, Ireland

²School of Civil and Environmental Engineering, Georgia Institute of Technology, Atlanta, GA

³School of Engineering and Architecture, University College Cork, Cork, Ireland

⁴School of Natural and Built Environment, Queen's University Belfast, Belfast, UK

⁵School of Architecture, Georgia Institute of Technology, Atlanta, GA

Corresponding Author:

Lawrence Bank, lbank3@gatech.edu

has been a developing body of research that has studied the issues of recycling and EOL of FRP composites, in general, and composite wind blades in particular. Recent analyses of the key issues related to the EOL of wind turbine blades can be found in Liu and Barlow (6), Jensen and Skelton (7), Cooperman et al. (8), Bank et al. (9), WindEurope (10), EPRI (11), and NCC (12). It is estimated that approximately 40 million tons of FRP blade waste will need to be disposed of by 2050 if no action is taken in the interim (3, 6).

A pedestrian bridge concept was identified by the Re-Wind Network in 2017 at the start of the research as a suitable application for repurposing blades. Early work on the concept and a preliminary design and analysis for an 8-m long pedestrian bridge using an A29 wind blade has been described in research by Suhail et al. (4). The Re-Wind Network calls this concept the “BladeBridge.” In early 2020, the University College Cork team became aware of extensive plans for the development of pedestrian and cycle ways in Ireland. The Irish Program for Government pledged 1 million euros per day on cycling and walking infrastructure, which included the construction of hundreds of pedestrian bridges. In mid-2020, the Re-Wind Network shared information with Cork County Council planners about the BladeBridge concept. The planners were interested in the sustainable nature of the bridge, and consequently chose to consider a BladeBridge for one of the planned greenway bridges. Munster Technological University (MTU) then requested and was granted seed funding through the MTU Research Office to support blade testing, and the detailed design and construction of a BladeBridge in their Structural Engineering Laboratory. The Georgia Tech (GT) team developed architectural renderings and structural models of possible concepts for the prototype bridge (Figure 1a). The BladeBridge, installed in January 2022 before final earthworks, is shown in Figure 1b.

In late 2020, the BladeBridge location was selected by the Middleton to Youghal Greenway project manager. The decision was made to build the bridge over a tributary of the Dungourney River in a prominent setting on the greenway. The location (Figure 2a) is 2 km from the start of the greenway at the Middleton railway station. The existing corroded steel beams were removed and the new BladeBridge was constructed over the river gap (currently a dry bed). The span is approximately 5 m with a 12° skew. Thirteen LM 13.4 blades used on Nordex N29 turbines (13, 14) manufactured in 1994 were donated by Everun (<https://everun.ltd>), a wind farm asset management company in Belfast, Northern Ireland. Eight blades were transported to MTU and five blades to Queen’s University Belfast (QUB). The blades were transported intact to the MTU Structural Engineering Laboratory. The 2.3-m long blade tips that served as aerodynamic

brakes on these early generation blades were removed before shipping. One blade was used for testing and another two were used in the bridge superstructure. Figure 2b shows one blade in the MTU structures laboratory yard.

The pedestrian and cycle bridge with dimensions of approximately 5 m long \times 3 m wide was designed according to the Eurocode (15). The dead (permanent) loads consist of the self-weight of the blade girders, a steel deck panels, cross-beams, and handrails. The static live (variable) load cases are (1) a uniformly distributed load, q_{fk} , of 5 kN/m² on the entire deck, and (2) the accidental 12 ton vehicle load case stipulated by the client. For the ultimate load analysis, the partial safety factors $\gamma_G = 1.35$ for dead (permanent) loads and $\gamma_Q = 1.5$ for live (variable) loads were used. In addition to this, a horizontal braking load at deck level, a concentrated load at the top of the handrail, and bridge natural frequency criteria, including user comfort criteria, stipulated by the code (15) were considered. The material partial factors for the design were taken from research by Ascione et al. (16), as described in a study undertaken by Gentry et al. (17). Fatigue loading is not required for a pedestrian bridge per the Eurocode (15), the AASHTO LRFD Guide Specifications for Pedestrian Bridges (18), or the AASHTO Guide Specifications for FRP Pedestrian Bridges (19). Creep was considered as per the Eurocode (15) and the AASHTO guide specification for FRP pedestrian bridges (19). Further details of the design process and the final design can be found in Zhang et al. (20).

Characterization of the LM 13.4 Wind Blade

Determination of Geometric and Material of the Wind Blade

The LM 13.4 has a length of 11 m when the brake at the tip of the blade is removed. The maximum chord length of the blade, measured from the leading- to the trailing edge, is located at 2.51 m from the root. To conduct the study of the blade’s physical and mechanical properties, the wind blade was cut into sections of approximately 1 m each. Figure 3 shows the side view and stations every meter along the wind blade length. Figure 4 shows details of the blade cross-section at Station 7.

Very few investigators have reported data for physical or mechanical properties of previously in-service and subsequently decommissioned wind blades (21–23). The LM 13.4 spar cap and shear webs are glass FRP as described in the Nordex N29/250 technical description and data (13, 14). Resin burnout tests were conducted in accordance with ASTM D2584 (24) to determine the laminate properties of the wind blade’s FRP material.

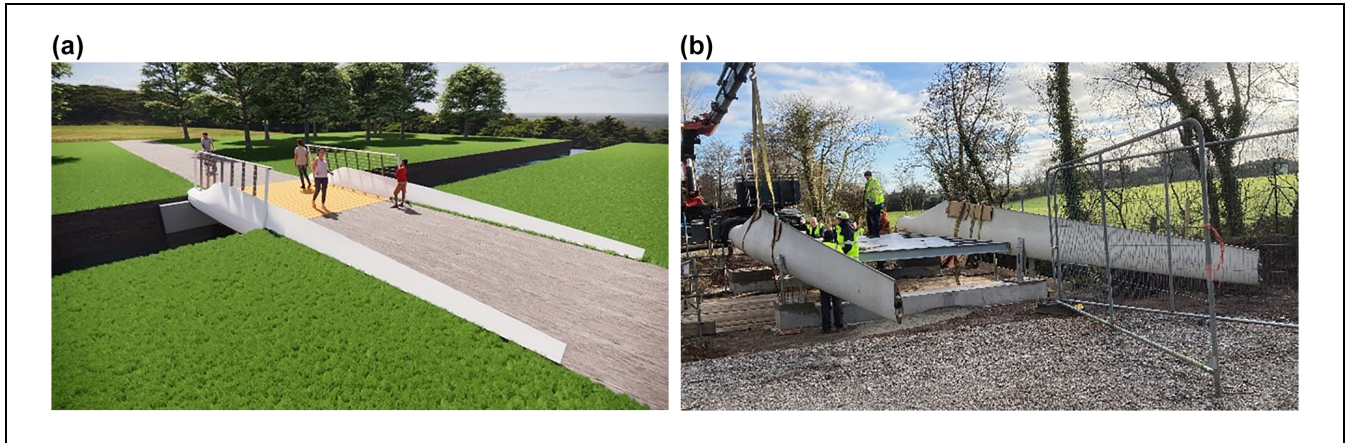


Figure 1. (a) Renderings of concepts for the Cork BladeBridge and (b) installed BladeBridge in Cork, Ireland.

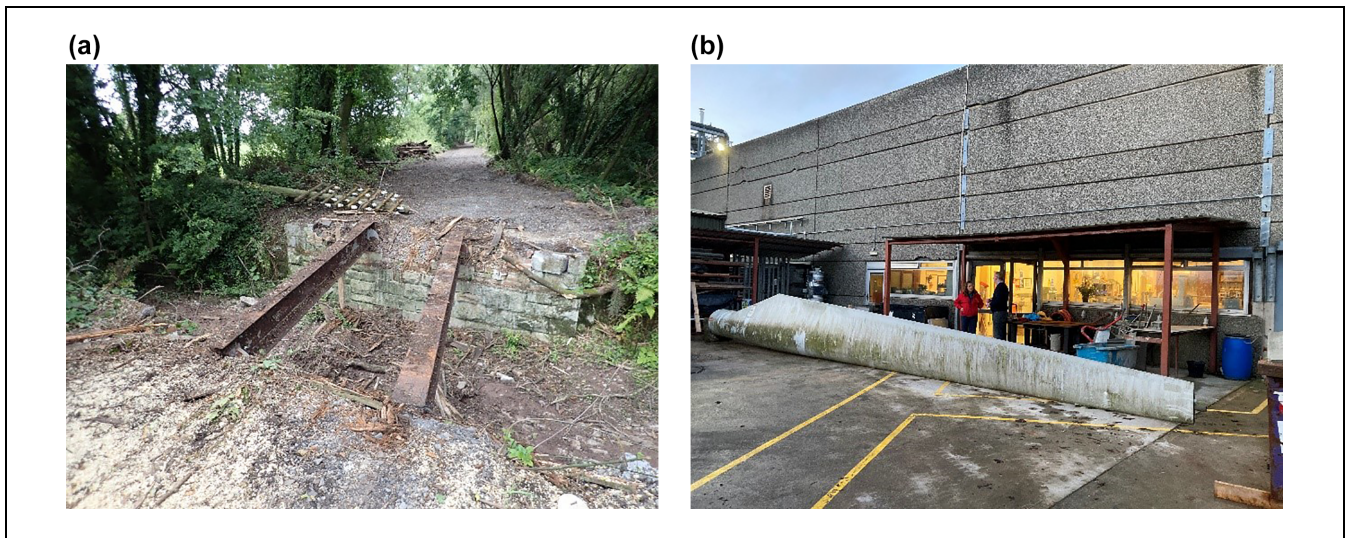


Figure 2. (a) Bridge site and (b) LM 13.4 blade on arrival at the Munster Technological University (MTU) structures laboratory yard.

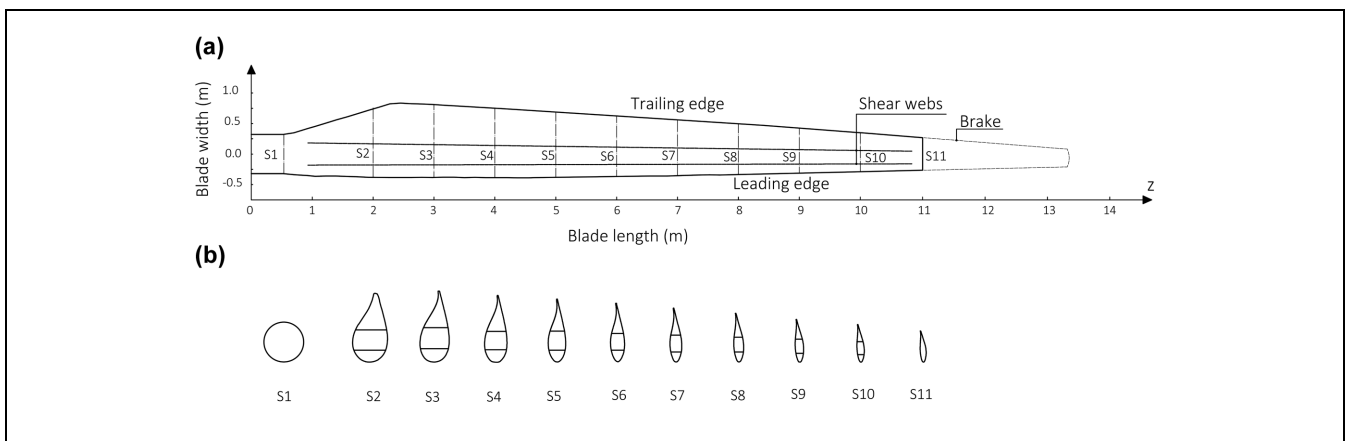


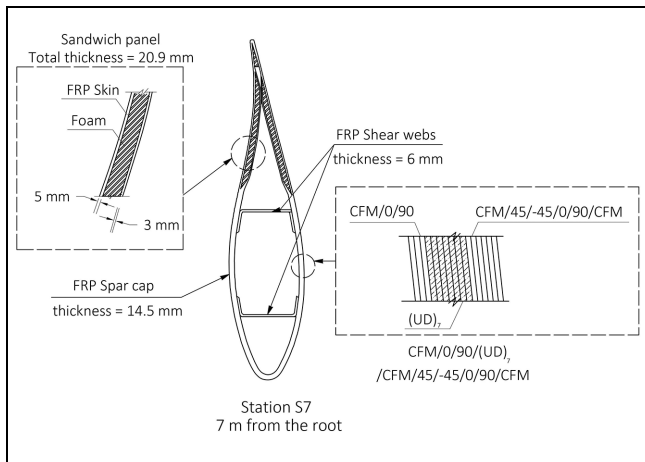
Figure 3. (a) Side view of the LM 13.4 blade and station numbering and (b) airfoil cross-sections at stations.

Table 1. Physical Properties Obtained from Burnout Testing of the Spar Cap and Shear Web of the LM 13.4 Wind Blade

Physical property	Wind blade component				
	Spar cap				Shear web Station 4
	Station 2	Station 4	Station 7	Station 10	
Fiber volume fraction	0.38–0.41	0.4–0.43	0.36–0.39	0.40–0.42	0.31–0.33
Stacking sequence (from outer surface to inner surface)	CFM/ ± 45/0-90/CFM/ (UD) ₁₀ /0-90/CFM	CFM/ ± 45/0-90/CFM/ (UD) ₉₋₁₃ ^a /0-90/CFM	CFM/ ± 45/0-90/CFM/ (UD) ₇ /0-90/CFM	CFM/ ± 45/0-90/ CFM/(UD) ₄ /0-90/CFM	(0-90/CFM) ₇

Note: CFM = continuous filament mat; ± 45 = balanced + 45/–45 fabric; UD = unidirectional fabric containing weft (90) fibers; 0-90 = balanced 0-90 fabric.

^aThe UD layers vary in number across the width of the panel.

**Figure 4.** Details of Station S7 in the LM 13.4 wind turbine blade.

Samples measuring approximately 25 mm × 50 mm were extracted from five stations (denoted by S2, S4, S7, S9, and S10 in Figure 3) and heated in a furnace at 565 ± 28°C until all carbonaceous material had disappeared. Initial and final weights were recorded to determine the fiber mass percent of each sample. This was converted to the volume fraction as per ASTM D3171 (25). Once the test was completed, each sample's fiber layers were carefully separated, photographed, and weighed, to determine the sample's laminate stacking sequence listed in Table 1.

The strength and longitudinal tensile modulus of the FRP composite extracted from the spar cap and shear webs at Station 4 were obtained from tensile and compressive tests in accordance with ASTM D3039 (26) and ASTM D3410 (27). The sandwich shells in the trailing edge panels of the blade were not tested at this time. Ultimate tensile and compressive strengths of the FRP composite were obtained. Coupons were cut from 250-mm long × 250-mm wide spar cap and shear web panels at Station 4. Because of the curved contour of the blade (see Figure 4), the coupons from the spar cap were obtained by removing the outer layers of the material to

give flat coupons containing only the unidirectional layers. Given that the shear web surfaces were already flat (see Figure 4), these coupons were cut directly from the panels. For tensile testing, the coupons were 250-mm long × 20-mm wide × 6 to 7-mm thick. For compressive testing, coupons were 155-mm long × 20-mm wide × 6 to 7-mm thick. Epoxy glass tabs were bonded at both ends of the specimens. The results of tests are shown in Table 2. Table 3 shows how these data compare with the very limited data from decommissioned wind blades that have been reported in the literature (21–23). Unfortunately, detailed values for volume fraction and coupon location were not always reported with these data. However, it can be seen that the data in Table 2 are similar in magnitude to those reported by others and are therefore felt to be reasonable for design purposes.

Determination of the Structural Properties of the Wind Blade

Details of the cross-section for calculation of the section properties at Station 7 are shown in Figure 5a. The standard wind blade nomenclature is used: LP—low pressure side; HP—high pressure side; LE—leading edge; TE—trailing edge. The analytical model does not include the low-modulus foam in the sandwich panels within the trailing edge panels that can be seen in green color Figure 5b. The composite section properties were calculated from the analytical model, which was created by LiDAR scanning of the blade and matching the scans with known airfoils in a proprietary software known as BladeMachine (28). This was augmented with thickness measurements and material property data taken from the blade. The wind blade was divided into eight zones for calculation of properties: (1) the leading edge web, (2) the trailing edge web, (3) the low pressure spar cap, (4) the low pressure leading edge shell, (5) the high pressure leading edge shell, (6) the high pressure spar cap, (7) the high pressure trailing edge, and (8) the low pressure trailing edge. The thickness and material properties of

Table 2. Mechanical Properties of the Spar Cap and Shear Web Obtained at Station 4 in the LM 13.4 Wind Blade

Mechanical property	Spar cap		Shear web	
	Number of specimens	Value	Number of specimens	Value
σ_t^{long} (MPa)	4	342 ± 19	5	207 ± 26
σ_c^{long} (MPa)	5	415 ± 29	5	164 ± 10
σ_t^{trans} (MPa)	5	16 ± 1	-	-
σ_c^{trans} (MPa)	4	72 ± 7	-	-
E_{long} (GPa)	1 ^a	27.5^a	1	10^a

Note: σ_t^{long} = longitudinal tensile strength; σ_c^{long} = longitudinal compressive strength; σ_t^{trans} = transverse tensile strength; σ_c^{trans} = transverse compressive strength; E_{long} = longitudinal tensile modulus.

^aMeasured with extensometer.

Table 3. Comparison of Mechanical Property Test Data with Literature

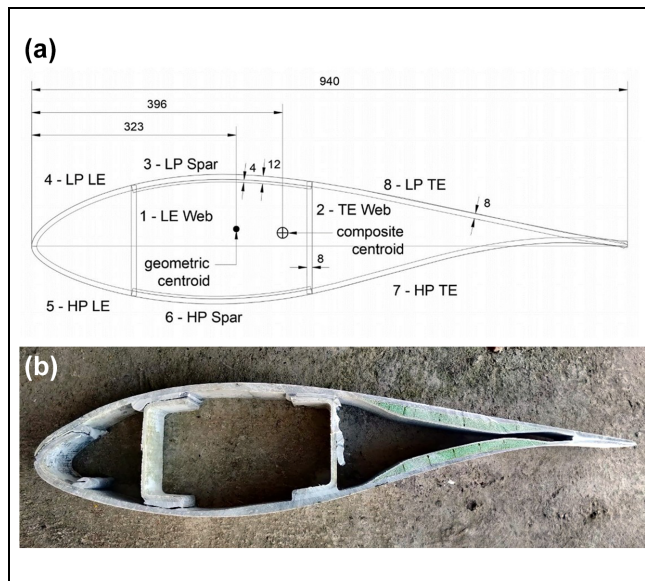
	Spar cap of N29 (LM13.4) ^a	Alshannaq et al. (21) ^b	Sayer et al. (22) ^c	Ahmed et al. (23) ^d
σ_t^{long} (MPa)	342	597	477	350
σ_c^{long} (MPa)	415	503	447	230
E_{long} (GPa)	27.5	36.8	26.7	15.6

^aThis paper: v_f = 35% to 43%.

^bAlshannaq et al. (21): spar cap of a 37 m long GE37 blade (v_f = 48%–50%).

^cSayer et al. (22): spar cap of DEBRA-25 blade (2.0 to 2.4 m from the root) with a total length of 11.6 m (similar to the N29 blade).

^dAhmed (23): spar cap of a 20 year-old wind blade (unidentified) with a total length of 9.8 m (similar to the N29 blade).

**Figure 5.** (a) Cross-section of the analytical model at Station 7 and (b) actual blade section at Station 7.

each of these zones were input into BladeMachine to determine the composite centroid and calculate the section properties.

The key properties for structural analysis of the wind blade used in this configuration were the edgewise

Table 4. Stiffnesses at Stations in the Test Specimen

Station	$(EI)_{yy}$ (N-m^2) $\times 10^6$	GA_s (N) $\times 10^7$
7	37.1	6.92
8	26.0	6.37
9	16.5	5.57
10	11.2	4.81
11	6.99	4.23

flexural stiffness, $(EI)_{yy}$, and the edgewise transverse shear stiffness, GA_s . The transverse shear stiffness, required to perform the deflection calculations that included shear deformation, was approximated as the projected height of the wind blade \times twice the average shell thickness of the blade at a given section. The flexural and shear stiffnesses vary as a function of length from the blade root, and this variation must be accounted for in the stress and deflection calculations.

The edgewise flexural and transverse shear stiffnesses at the stations used in the full-scale specimen are given in Table 4. The longitudinal moduli used for the shell, the spar cap, and the web were 27.5, 27.5, and 10.0 GPa, respectively, as reported in Table 1. A shear modulus of 4.6 GPa was assumed for all parts (i.e., the shell, the webs, and the spar caps). Future testing will include shear tests on the LM 13.4 as well as additional repeats

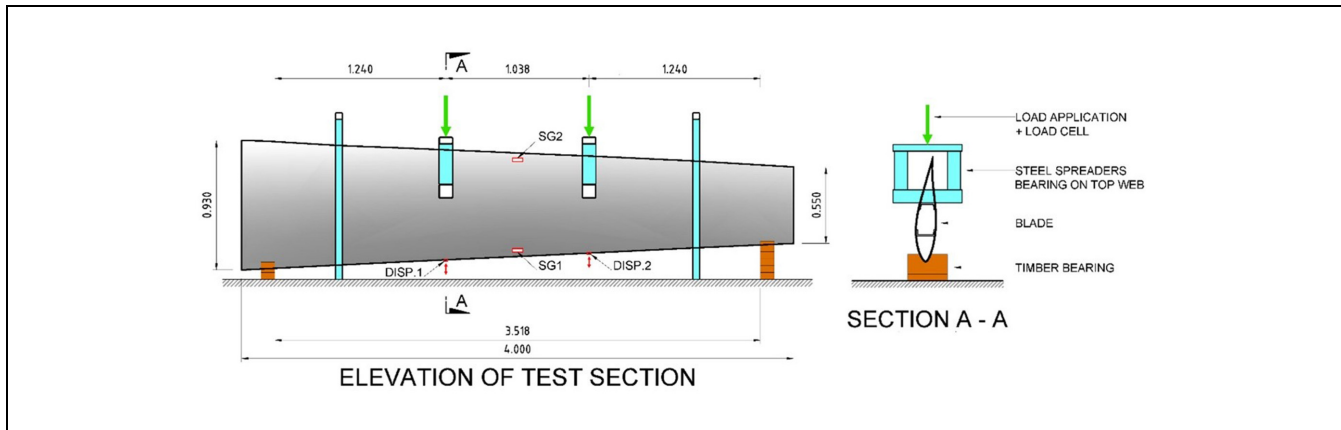


Figure 6. Test fixture dimensions and details.

of the other mechanical tests. The thickness of the shell for the model was taken as 8 mm for all stations, however, to account for the extra thickness in the spar cap region, 4, 3, 2, 1, and 0 mm were added to the 8-mm shell for Stations 7, 8, 9, 10, and 11 respectively. The thickness of the shear webs were taken as 8 mm.

Determination of the Load-Deflection Behavior of the Blade in Edgewise Bending

The large load test rig at the Structural Engineering Laboratory at MTU was used to conduct a four-point bending test of a 4-m long section of the blade from Stations 7 to 11 (shown in Figure 3a) in edgewise bending. This was the largest section capable of being tested in the test frame. For the actual bridge design, the stiffer and stronger section from Stations 0 to 5 were used, as shown in Figures 1b and 3. The large load test rig at MTU can apply vertical loads up to a total magnitude of 1,000 kN. The blade section was oriented in accordance with the conceptual design of the BladeBridge such that the leading edge of the blade was at the bottom, webs were kept horizontal, and the chord axis was vertical as shown in Figure 1, a and b. The blade was placed in light-gauge steel frames complete with timber wedges to maintain lateral stability of the test specimen under load application as shown in Figures 6 and 7. Timber bearing pads were cut to the profile of the blade to serve as supports for the blade beam. The clear distance between the face of the supports was 3.52 m. Load was applied to the test specimen by a spreader beam system under each hydraulic jack with slots cut in the skin of the blade such that the spreader beam system applied load directly to the upper (TE) web of the test specimen. Vertical deflection (DISP 1 and DISP 2) was recorded using linear variable differential transformers (LVDTs) placed under the blade beam at the points of load application. Lateral

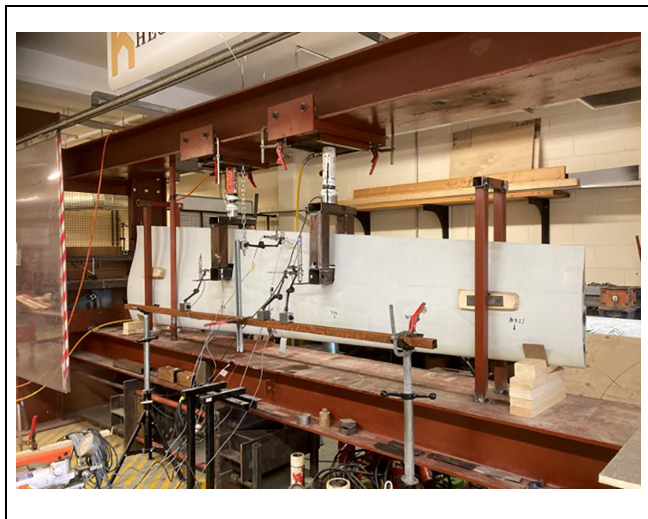


Figure 7. Test rig with wind blade test specimen in the laboratory.

displacement of the compression face of the blade beam was recorded at midspan with LVDTs. Strain gauges (SG1 and SG2) oriented in the longitudinal direction were bonded to the skin of the specimen at midspan. Load cells were provided under each hydraulic jack and all instrumentation was logged with a multichannel data acquisition monitoring system operating at a sampling frequency of 10 Hz across all instruments.

The load versus deflection plots at DISP 1 and DISP 2 are shown in Figure 8, a and b. The maximum total load sustained by the test sample was 87.2 kN (equivalent applied moment 54.1 kN-m) with an associated vertical displacement (averaged) at the loading points of 18.5 mm. The load-deflection history of the test is complex and key stages are as follows: after an initial period of bedding-in of the sample on the timber bearings, the load was increased gradually to approximately 65 kN

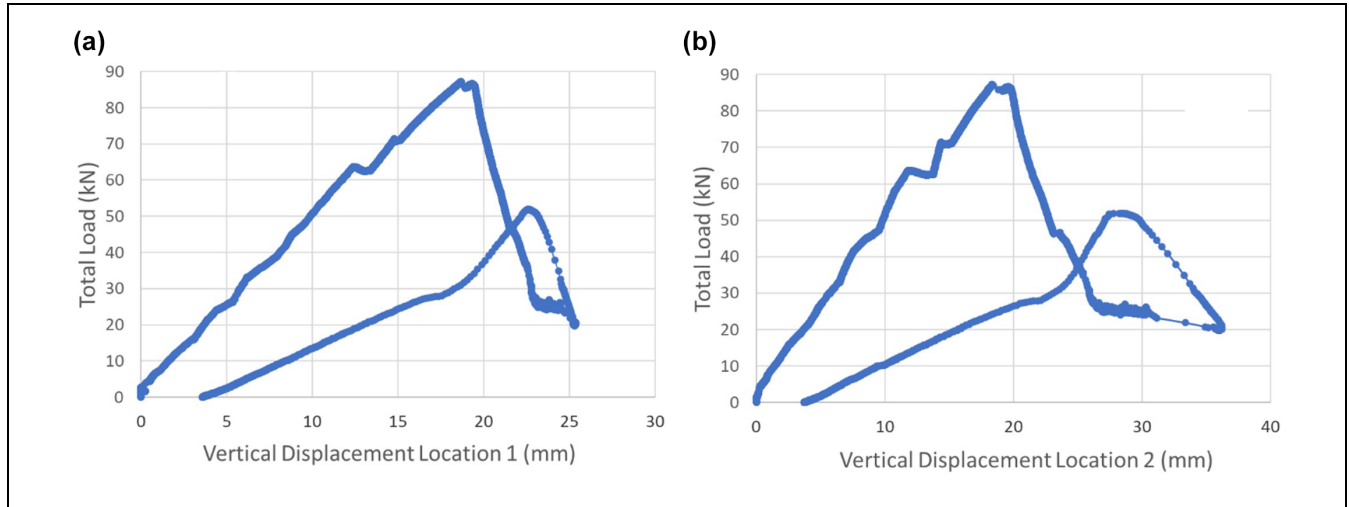


Figure 8. (a) Load versus deflection at Location 1 and (b) load versus deflection at Location 2.

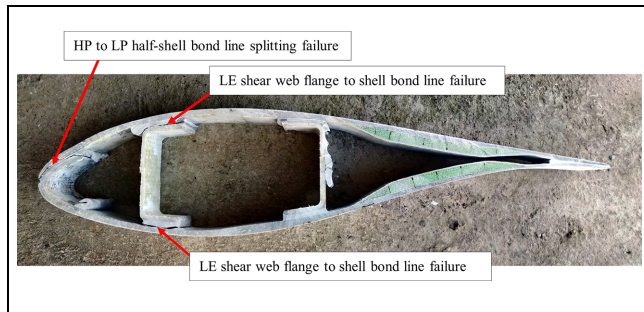


Figure 9. Station 7 after sectioning at completion of the test showing failure locations.

and held with the sample demonstrating linear-elastic behavior. As the load was held, the sample continued to deflect. When the deflection ceased, the load was increased to 70 kN and again held with the sample continuing to deflect. Once this deflection had ceased, the load was increased until failure, which was characterized by an explosive sound, a minor load reduction, and further deflection. The sound was attributed to the separation of the shear web flanges from the skin at the bottom (LE) shear web and the splitting of the bottom (LE) of the blade half-shells in the area of the supports (see Figure 9). At this point the specimen was severely damaged. The test load was reduced to approximately 25 kN and held. Deflection continued to 30.7 mm (average) as progressive failure propagated through the specimen. Though the specimen was significantly damaged at this point, load was increased to 50 kN to examine its residual integrity. Load redistribution in the specimen during this reloading phase was complex owing to the extent of damage to the beam, and the LVDTs recorded a reduction in deflection at the load points (attributed to

crushing at the left-hand support). A further explosive sound (attributed to longitudinal splitting at the leading edge) was heard and the sample was then fully unloaded. The residual deflection was 3.7 mm (average).

Discussion

The experimental investigation of the wind turbine blade revealed several important items that contributed to the design of the bridge. Based on the material testing, the FRP material appeared to be in excellent condition. No defects or delaminated regions were seen. The fiber layup was easy to determine and the fabric type easy to identify. Fiber volume fractions were consistent with the manufacturing methods used for blades of this generation. The full-scale test showed linear-elastic behavior up until failure and then a progressive failure after the peak load. The initial failure occurred at the connection between the shear web flanges and the outer shell. This was followed by a splitting failure at the leading edge of the wind blade (the girder bottom in the test) where the two half-shells were bonded together when manufactured. The full-scale testing revealed the importance of building a stiff diaphragm at the supports and securing the web flanges to the shell.

Future Work

Connection tests of the floor beams to the blade were also conducted and will be reported elsewhere. Creep testing on the full-scale bridge prototype will be performed before opening the bridge to the public. Additional material coupon tests, including ASTM fatigue tests and creep tests, will also be conducted to determine long-term performance of the material. The

BladeBridge will be instrumented and monitored in situ and the results reported in the future.

Conclusions

The results of the studies reported to characterize an LM 13.4 wind blade were used by the bridge engineers to design and analyze the bridge, as well as to develop the details, specifications, and construction methods needed for the Middleton to Youghal Greenway BladeBridge that was constructed in County Cork, Ireland in January 2022.

Acknowledgments

This work would not have been possible without support from other faculty, students, and staff in the Re-Wind Network at our partner institutions including Conor Graham, Emma Delaney, Kenny McDonald of QUB; Tristan Al-Haddad, Chloe Kiernicki, Mehmet Bermek, Sakshi Kakkad of GT; and Maggie Shorten, Jim Morgan, Liam Jones of MTU.

Author Contributions

The authors confirm contribution to the paper as follows: study conception and design: P. Leahy, A. Nagle, K. Ruane, L. Bank, R. Gentry, M. Soutsos, J. McKinley; data collection: K. Ruane, L. Bank, R. Gentry, A. Alshannaq, A. Huynh, Z. Zhang; analysis and interpretation of results: K. Ruane, L. Bank, R. Gentry, A. Alshannaq, A. Huynh, Z. Zhang; draft manuscript preparation: K. Ruane, L. Bank, R. Gentry, A. Alshannaq, A. Huynh, Z. Zhang, A. Nagle, P. Leahy, A. McDonald. All authors reviewed the results and approved the final version of the manuscript.





Declaration of Conflicting Interests





The authors declared no potential conflicts of interest with respect to the research, authorship, and/or publication of this article.

Funding

The authors disclosed receipt of the following financial support for the research, authorship, and/or publication of this article: This research was funded by the U.S. National Science Foundation under grants 2016409, 1701413, and 1701694; by InvestNI/Department for the Economy under grant 16/US/3334 and by Science Foundation Ireland under grant USI-116 as part of the U.S.–Ireland Tripartite research program. Grant support from the MTU Research Office and blade donation from Everun, Ltd. is also acknowledged

ORCID iDs

Zoe Zhang  <https://orcid.org/0000-0003-4726-4946>
 Angela Nagle  <https://orcid.org/0000-0001-8790-4341>
 An Huynh  <https://orcid.org/0000-0003-0416-9463>
 Ammar Alshannaq  <https://orcid.org/0000-0002-3455-3784>

Paul Leahy  <https://orcid.org/0000-0003-4478-3863>
 Marios Soutsos  <https://orcid.org/0000-0001-5235-2196>
 Jennifer McKinley  <https://orcid.org/0000-0003-2327-5560>
 Lawrence Bank  <https://orcid.org/0000-0002-4279-4473>

References

- Nicholl, M., L. Bank, J.-F. Chen, R. Gentry, P. Leahy, A. Nagle, B. Tasistro-Hart, et al. *Re-Wind Design Atlas*, 2018. <https://static1.squarespace.com/static/5b324c409772ae52fecb6698/t/5f2ac069ea2995235ee57b85/1596637300551/Re-Wind+Design+Atlas+V1+Nov+2018+licensed+under+%28CC+BY-NC-SA+4.0%29.pdf>. Accessed January 28, 2022.
- McDonald, A., C. Kiernicki, M. Bermek, Z. Zhang, A. Poff, S. Kakkad, E. Lau, F. Arias, R. Gentry, and L. C. Bank. *Re-Wind Design Catalog Fall*, 2021. <https://static1.squarespace.com/static/5b324c409772ae52fecb6698/t/61e95d5f4ef3ad0d5eddd595/1642683746379/Re-Wind+Design+Catalog+Fall+2021+Nov+12+2021+%28low+res%29.pdf>. Accessed January 28, 2022.
- Bank, L. C., F. R. Arias, A. Yazdanbakhsh, T. R. Gentry, T. Al-Haddad, J.-F. Chen, and R. Morrow. Concepts for Reusing Composite Materials from Decommissioned Wind Turbine Blades in Affordable Housing. *Recycling*, Vol. 3, 2018, p. 3.
- Suhail, R., J.-F. Chen, T. R. Gentry, B. Tasistro-Hart, Y. Xue, and L. C. Bank. Analysis and Design of a Pedestrian Bridge with Decommissioned FRP Windblades and Concrete. *Proc., 14th International Symposium on Fiber-Reinforced Polymer Reinforcement of Concrete Structures*, Belfast, UK, 2019.
- Alshannaq, A. A., L. C. Bank, D. W. Scott, and T. R. Gentry. Structural Analysis of a Wind Turbine Blade Repurposed as an Electrical Transmission Pole. *ASCE Journal of Composites for Construction*, Vol. 25, 2021, p. 04021023.
- Liu, P., and C. Y. Barlow. Wind Turbine Blade Waste in 2050. *Waste Management*, Vol. 62, 2017, pp. 229–240.
- Jensen, J. P., and K. Skelton. Wind Turbine Blade Recycling: Experiences, Challenges and Possibilities in a Circular Economy. *Renewable and Sustainable Energy Reviews*, Vol. 97, 2018, pp. 165–176.
- Cooperman, A., A. Eberle, and E. Lantz. Wind Turbine Blade Material in the United States: Quantities, Costs, and End-of-Life Options. *Resources, Conservation and Recycling*, Vol. 168, 2021, p. 105439.
- Bank, L. C., R. Gentry, E. Delaney, J. McKinley, and P. Leahy. Defining the Landscape for Wind Blades at the End of Their Service Life. *CompositesWorld*, Vol. 7, 2021, pp. 6–9.
- WindEurope. *Accelerating Wind Turbine Blade Circularity*. 2020. <https://windeurope.org/wp-content/uploads/files/about-wind/reports/WindEurope-Accelerating-wind-turbine-blade-circularity.pdf>. Accessed January 28, 2022.
- EPRI. *Wind Turbine Blade Recycling: Preliminary Assessment*. Report 3002017711. EPRI, Palo Alto, CA, 2020. <https://www.epri.com/research/products/00000003002017711>. Accessed January 28, 2022.

12. NCC. *Sustainable Decommissioning: Wind Turbine Blade Recycling*, 2021. Report from Phase 1 of the Energy Transition Alliance Blade Recycling Project. https://ore.catapult.org.uk/wp-content/uploads/2021/03/CORE_Full_Blade_Report_web.pdf. Accessed January 28, 2022.
13. Nordex N29/250 Datasheet. <https://en.wind-turbine-models.com/turbines/56-nordex-n29>. Accessed January 28, 2022.
14. *Nordex N29/250 Technical Description and Technical Data*. Nordex Windkraftanlagen, Svindbaek, Denmark, 1994.
15. IS, EN 1991-2:2003 + NA:2009. *Eurocode 1: Actions on Structures – Part 2: Traffic loads on bridges* (Inc. National Annex to IS EN 1991-2:2003) The National Standards Authority of Ireland, Dublin, Ireland, 2009.
16. Ascione, L., J. F. Caron, J. R. Correia, W. De Corte, P. Godonou, J. Knippers, E. Moussiaux, et al. *Prospect for New Guidance in the Design of FRP Structures*. EuCIA, Brussels, Belgium, 2017. <https://tinyurl.com/2udjvn7y> and at <https://eucia.eu/publications/>. Accessed January 28, 2022.
17. Gentry, T. R., T. Al-Haddad, L. C. Bank, F. R. Arias, A. Nagle, and P. G. Leahy. Structural Analysis of a Roof Extracted from a Wind Turbine Blade. *ASCE Journal of Architectural Engineering*, Vol. 26, No. 4, 2020, p. 04020040.
18. American Association of State Highway and Transportation Officials. *LRFD Guide Specifications for the Design of Pedestrian Bridges*. Washington, DC: AASHTO, 2009.
19. American Association of State Highway and Transportation Officials. *Guide Specifications for the Design of FRP Pedestrian Bridges*. Washington, DC: AASHTO, 2008.
20. Zhang, Z., K. Ruane, A. Huynh, A. McDonald, P. Leahy, A. Alshannaq, T. R. Gentry, A. Nagle, and L. C. Bank. BladeBridge - Design and Construction of a Pedestrian Bridge Using Decommissioned Wind Turbine Blades. *Proc., 5th the International Conference on Structures and Architecture*, Aalborg, Denmark, 2022.
21. Alshannaq, A., J. Respert, L. Bank, D. Scott, and R. Gentry. As-Received Physical and Mechanical Properties of the Spar Cap of a GE37 Decommissioned Glass FRP Wind Turbine Blade. *ASCE Journal of Materials in Civil Engineering*, 2022. (in production)
22. Sayer, F., F. Bürkner, B. Buchholz, M. Strobel, A. M. van Wingerde, H. G. Busmann, and H. Seifert. Influence of a Wind Turbine Service Life on the Mechanical Properties of the Material and the Blade. *Wind Energy*, Vol. 16, No. 2, 2013, pp. 163–174.
23. Ahmed, M. M., B. Alzahrani, N. Jouini, M. M. Hessian, and S. Ataya. The Role of Orientation and Temperature on the Mechanical Properties of a 20 Years Old Wind Turbine Blade GFR Composite. *Polymers*, Vol. 13, No. 7, 2021, p. 1144.
24. ASTM D2584. *Standard Test Method for Ignition Loss of Cured Reinforced Resins*. ASTM International, West Conshohocken, PA, 2011.
25. ASTM D3171. *Standard Test Methods for Constituent Content of Composite Materials*. ASTM International, West Conshohocken, PA, 2015.
26. ASTM D3039/D3039M. *Standard Test Method for Tensile Properties of Polymer Matrix Composite Materials*. ASTM International, West Conshohocken, PA, 2017.
27. ASTM D3410/D3410M. *Standard Test Method for Compressive Properties of Polymer Matrix Composite Materials with Unsupported Gage Section by Shear*. ASTM International, West Conshohocken, PA, 2016.
28. Tasistro-Hart, B., T. Al-Haddad, L. C. Bank, and R. Gentry. Reconstruction of Wind Turbine Blade Geometry and Internal Structure from Point Cloud Data. *Proc., ASCE International Conference on Computing in Civil Engineering*, Atlanta, GA, 2019.